

Illumination Analysis of Halogen Compared with Manganese Cobalt Composite Material Using Novel Sol-gel Method

Rayachoty Bhaskar and Karthik Poornachandran*

Department of Mechanical Engineering, Saveetha School of Engineering, Saveetha Institute of Medical and Technical Sciences, Saveetha University, Chennai, Tamil Nadu, India

*Correspondence to:

Karthik Poornachandran
Department of Mechanical Engineering,
Saveetha School of Engineering,
Saveetha Institute of Medical and Technical Sciences,
Saveetha University,
Chennai, Tamil Nadu, India.
E-mail: karthikp.sse@saveetha.com

Received: July 26, 2023

Accepted: September 27, 2023

Published: October 03, 2023

Citation: Bhaskar R, Poornachandran K. 2023. Illumination Analysis of Halogen Compared with Manganese Cobalt Composite Material Using Novel Sol-gel Method. *NanoWorld J* 9(S3): S110-S114.

Copyright: © 2023 Bhaskar and Poornachandran. This is an Open Access article distributed under the terms of the Creative Commons Attribution 4.0 International License (CCBY) (<http://creativecommons.org/licenses/by/4.0/>) which permits commercial use, including reproduction, adaptation, and distribution of the article provided the original author and source are credited.

Published by United Scientific Group

Abstract

The objective of this study was to compare the illumination properties of halogen with a manganese cobalt (Mn-Co) composite material using a novel sol-gel method. The manganese and cobalt were doped using the sol-gel method to prepare the composite material. Gradual addition of ethanol was done to remove negative ions from the composite. The illumination characteristics of the Mn-Co composite material were evaluated using XRD (X-ray diffraction), SEM (Scanning electron microscope), and UV-Vis (Ultraviolet-Visible) testing methods. Two groups were selected for the investigation of the UV-Vis absorption spectrum: Group 1 - Halogen at the activation temperature of 1000 °C, and Group 2 - Mn-Co composite material at the peak activation temperature of 1000 °C. Each group consisted of 20 samples, determined based on a pretest power of 80%, a probability value of 0.05%, and a confidence interval (CI) of 95%. A complete of 2 specimens were divided into a pair of teams with G-power of 80. The research findings indicated that the particle size of the Mn-Co composite material increased with the rise in temperature, and the peak absorbance wavelength decreased with increasing particle size. The results revealed a statistically significant difference between the two groups, with a p-value of 0.000 ($p < 0.05$). The analysis focused on examining the crystal structure of the composite material, phase purity, and optical properties. The band gap (eV) (0.7370 mm³/sec) of Mn-Co nanoparticles mean was found to be 0.3568 mm³/sec, which is higher than that of normal illumination. This study concluded that the Mn-Co composite material provides enhanced illumination compared to halogen material, which only provides normal illumination. The sol-gel method allowed for the efficient doping of manganese and cobalt in the composite, leading to improved illumination properties. The findings from this research could have significant implications in the development of advanced lighting materials for various applications.

Keywords

Halogen, Manganese, Cobalt, Composite material, Sol-gel method, Optical property, Nanoparticles, Natural resources, Carbon

Introduction

This study aims to investigate the optical characteristics of a composite material developed using the sol-gel method, which differ significantly from those of bulk metal oxide nanoparticles and have recently gained considerable attention in research [1]. Manganese exhibits various oxidation states, making the formation of different manganese oxides possible, adding to the versatility of the composite material [2]. The unique magnetic properties of manganese oxide composite material nanoparticles, resulting from their high manganese atomic moment and diverse magnetic alignment, have become a subject of growing scientific interest [3]. In the field of waste gas treatment, polymorphs of manganese doped cobalt

have been effectively utilized as catalysts to remove harmful pollutants such as carbon monoxide and nitrogen oxide through a dip coating method [4]. This highlights the potential applications of composite material in various industries, including the automobile sector and chemical industry. Overall, this study will shed light on the optical characteristics and potential applications of the composite material developed using the sol-gel method, showcasing its distinct properties and promising role in various scientific and industrial domains [1-4]. Aerospace and among others these materials are used for a variety of purposes [5].

The subject of this study has a substantial body of related research, with 7,056 similar works available in Google Scholar and 610 works available in Science Direct. Within this context, nanosized Mn_2O_3 is of particular interest due to its smaller grain size and larger surface area, which are expected to enhance its performance in various applications [6]. Notably, nanosized Mn_2O_3 finds applications in the creation of soft magnetic materials like manganese and cobalt, which are crucial components in the magnetic cores of power supply transformers. Additionally, it is utilized in the production of fluxes and welding rods. Furthermore, nanosized Mn_2O_3 serves as an essential raw material in the production of high-quality ferrites [5]. Given the abundance of research and the diverse applications of nanosized Mn_2O_3 , this study is poised to contribute valuable insights into its optical characteristics and potential uses, building upon the existing knowledge base [5, 6].

Up to this point, no research has been conducted using the novel powdered nanocrystalline Mn_2O_3 composite material. However, various processes, such as hydrothermal, thermochemical, spray pyrolysis, chemical liquid homogeneous precipitation, thermal breakdown, and arc evaporation methods, have been utilized to produce nanocrystalline Mn_2O_3 composite materials [7]. The material's suitability for use in magnetic storage relies on its ferromagnetic properties. Cobalt is typically an antiferromagnetic material with a Curie temperature of 90 K and a Neel temperature of 90 K. However, when combined with tiny manganese particles and heated in ethanol, various combinations of Mn-Co exhibit ferromagnetic characteristics. This has sparked significant interest in the study of cobalt doped manganese. To explore the synthesis and characterization of cobalt doped manganese nano systems and their optical features, this research employs the auto combustion sol-gel technique [8]. Through this innovative approach, the study aims to shed light on the unique properties and potential applications of the synthesized nanocrystalline Mn_2O_3 composite material, offering valuable insights into its optical characteristics and suitability for various scientific and technological endeavors.

Materials and Method

This study was carried out in the Department of Mechanical Engineering at Saveetha School of Engineering, SIMATS, Chennai (Tamil Nadu, India). The researchers used halogen coating and deionized water as starting materials in their experiments [7]. To synthesize the nanocrystalline Mn_2O_3 composite material, an amber solution was prepared and heated

to 323 K while being stirred for an hour. After completing the stirring process, the solution was allowed to cool at room temperature, resulting in the formation of a dark brown precipitate [9]. To further purify the precipitate and remove any excess surfactant from the solution, centrifugation and multiple washes with distilled water or acetone were carried out [10]. Subsequently, the resulting material was dried in air for 30 min at 353 K.

Indeed, the specific techniques and procedures employed in this study aimed to synthesize the nanocrystalline Mn_2O_3 composite material successfully and obtain a purified and well-characterized product for further investigation [7, 9, 10]. The use of halogen coating and deionized water as starting materials, along with the controlled heating and stirring of the amber solution, resulted in the formation of a dark brown precipitate. Subsequent centrifugation and multiple washes with distilled water or acetone ensured the removal of any extra surfactant from the solution. By following these steps, the researchers aimed to produce a high-quality nanocrystalline Mn_2O_3 composite material with specific characteristics that can be studied and analyzed further. The purified product would enable the researchers to investigate its optical properties, magnetic behavior, and other relevant characteristics in detail, contributing valuable insights to the scientific understanding of this material's potential applications.

In this study, cobalt oxide composite materials of natural resources were mixed with the yield obtained separately using the microemulsion process in various amounts (0, 1, 2, 5, and 10 wt.%). The resulting mixture was thoroughly ground before being subjected to air-annealing for three hours at 700 K. The powder produced through the sol-gel method was then used for characterization [11]. For each group, 20 samples were taken to calculate the optical properties. The samples were divided into two teams, and a total of 40 specimens were used for analysis, employing the G-power calculator to ensure appropriate statistical power [11]. The analysis in this paper involves two different methods: (1) Optical band gap measurement of the manganese-doped zinc oxide, and (2) SEM analysis. These methods are utilized to examine and understand the optical and microstructural properties of synthesized materials [11]. The findings from this study will contribute valuable information to the field of nanomaterials and further our understanding of the potential applications of manganese-doped zinc oxide composites.

Statistical analysis

In this study, a t-test was conducted using the Statistical Package for the Social Sciences statistical program to analyze the relationship between the activation energy and band gap with varying manganese doping concentrations in the research samples. The activation energy was treated as the dependent variable, while the band gap, lattice cell, interplanar spacing, and unit cell volume of cobalt doped manganese nanoparticles in each sample were considered as independent variables. By performing the t-test, the researchers aimed to determine if there were statistically significant differences in the activation energy with respect to the different independent variables, which could provide valuable insights into the effect of

manganese doping concentration on the optical and structural properties of the cobalt nanoparticles. The results of this analysis would contribute to a deeper understanding of the behavior and characteristics of the cobalt doped manganese nanoparticles and their potential applications in various fields.

Results

The crystal structure of the materials phase purity optical characteristics was looked at. The XRD patterns of cobalt doped Mn_2O_3 nanosystems with varying doping concentrations of 0, 1, 2, 5, and 10 wt.% are shown in figure 1. The 10 wt.% cobalt doped manganese XRD pattern reveals that the crystalline peaks correspond to manganese in addition to the appearance of a secondary phase that corresponds to the orientation of cobalt, which may be caused by an increase in cobalt ion concentration above the solubility limit. The band gap energies of the Mn:Co vary between 3.34 eV and 3.22 eV. With a p-value of 0.000 ($p < 0.05$), these findings demonstrated a statistically significant difference between the two groups.

The high-resolution pictures of cobalt doped manganese nanoparticles (with $x = 0.0, 0.2, 0.4,$ and 0.6) obtained by SEM are shown in figure 2. The nanocrystalline character of the cobalt is shown by the ferrite grains, which range in size from 15.6 to 20 nm. Figure 1 illustrates how the distinctive XRD pattern of a particular phase can be used to assess the material's degree of crystallinity and phase purity. Cobalt doped manganese nanoparticles yielded XRD patterns that demonstrated the production of a homogenous single phase with a cubic spinel structure up to a manganese composition of 0.2.

Figure 3 shows the graphical depiction of band gap (eV) for group-1 (Manganese (2%), cobalt (1%), and group-2 (Mn-Co), with material groups on the X axis and band gap (eV) on the Y axis. The functional groups of cobalt doped manganese nanoparticles are shown in table 1. The results are generally consistent with the literature. Peaks at 500 and 600 cm^{-1} denote the manganese stretching mode. Table 2 shows how the band gap varies when group 1 and group 2 are doped with varying amounts of manganese while also calculating the band gap values using UV-Vis spectroscopy. Table 3 presents group statistics on band gap (eV) values for the groups. Table 4 presents an independent t-test for equality of means of the band gap (eV) values for the group.

Discussion

In this study, the materials were subjected to XRD analysis to investigate their optical characteristics, crystal structure, and phase purity. Figure 1 presents the XRD patterns of cobalt doped manganese nanosystems with different levels of doping. The results indicate a cubic structure, evident from the comparison of the diffraction peaks with the reference file. The lattice parameter, derived from the XRD data, was found to be $a = 9.408$, and it closely agrees with the JCPDS data and previous findings. The crystalline peaks observed in the XRD pattern for the 10 wt.% cobalt doped manganese sample are indicative of the presence of manganese. However, an increase in cobalt ion concentration above the solubility limit and the emergence of a secondary phase with cobalt's orientation may impact the

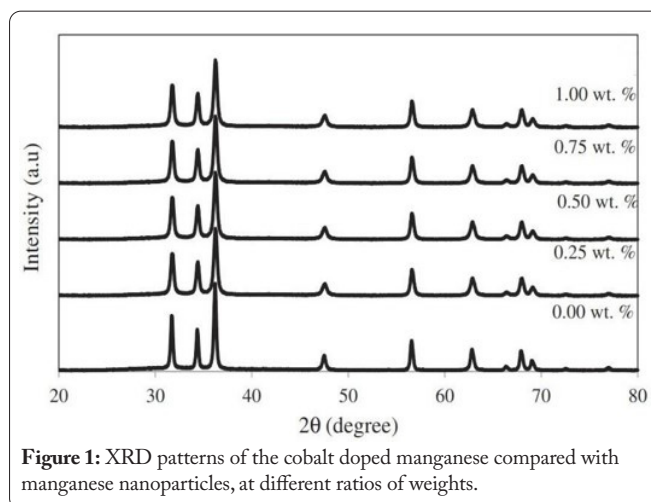


Figure 1: XRD patterns of the cobalt doped manganese compared with manganese nanoparticles, at different ratios of weights.

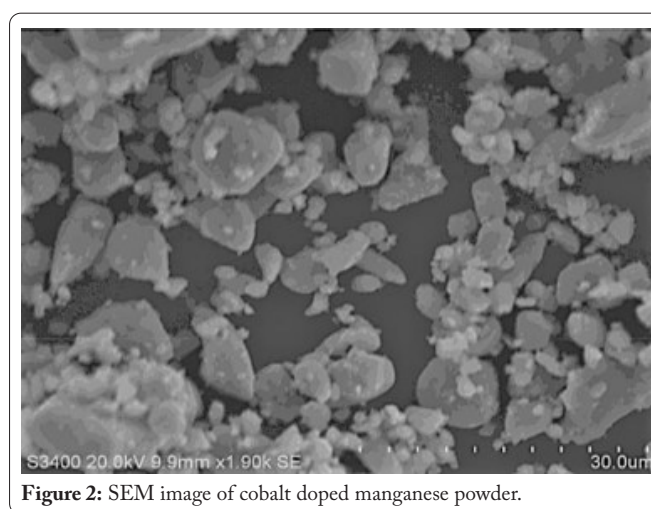


Figure 2: SEM image of cobalt doped manganese powder.

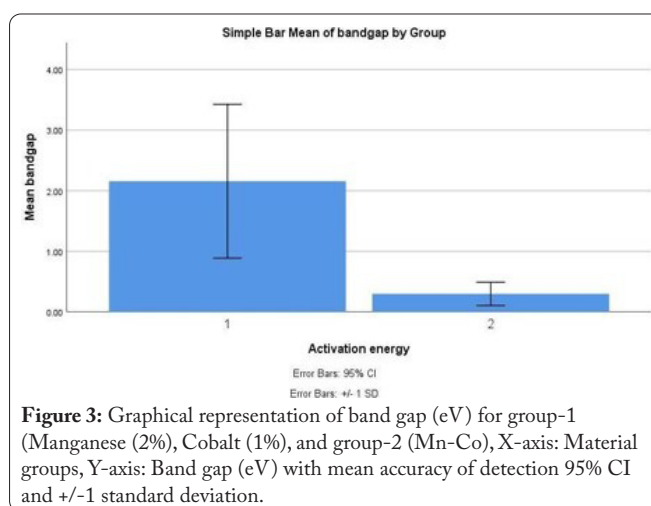


Figure 3: Graphical representation of band gap (eV) for group-1 (Manganese (2%), Cobalt (1%), and group-2 (Mn-Co), X-axis: Material groups, Y-axis: Band gap (eV) with mean accuracy of detection 95% CI and +/-1 standard deviation.

Table 1: Input parameters and their levels for elemental composition of synthesized nanoparticles of Mn-Co as evaluated from UV-Vis spectroscopy.

Parameters	Levels		
	L1	L2	L3
Samples	X = 0.0	X = 2.3	X = 3.5
Mn (Wt.%)	9.87	5.28	0.83
Co (Wt.%)	8.45	4.64	0.09

Table 2: Variation of band gap with cobalt doping manganese concentration of group 1 and group 2.

S. No.	Parameters			Group 1	Group 2
	Sam- ples	Mn (Wt.%)	Co (Wt.%)	Band gap (eV)	Band gap (eV)
1	0.0	9.87	8.45	3.97	0.38
2	0.3	9.73	8.12	3.82	0.28
3	0.5	8.65	7.45	3.75	0.49
4	0.8	8.34	7.16	3.61	0.54
5	1.0	7.56	6.45	3.57	0.31
6	1.3	7.23	6.78	2.90	0.46
7	1.5	6.87	5.41	2.82	0.35
8	1.8	6.12	5.21	2.77	0.26
9	2.0	5.45	4.78	2.64	0.42
10	2.3	5.28	4.64	2.30	0.50
11	2.5	4.67	3.54	1.97	0.32
12	2.8	4.74	3.41	1.83	0.64
13	3.0	3.12	2.53	1.81	0.44
14	3.3	3.26	2.32	1.72	0.15
15	3.5	2.89	1.75	1.55	0.25
16	3.8	2.78	1.34	0.9	0.02
17	4.0	1.47	0.12	0.5	0.04
18	4.3	1.54	0.32	0.4	0.09
19	4.5	0.13	0.02	0.2	0.02
20	4.8	0.83	0.09	0.1	0.001

Table 3: Group statistics on band gap (eV) values for the groups.

Group		N	Mean	Std. deviation	Std. error mean
Band gap (eV)	Lattice parameter (Group 1)	20	0.7570	0.88610	0.19814
	Inter planar spacing (Group-2)	20	0.3685	0.12424	0.02778

crystalline peaks and diffraction pattern [12]. The XRD analysis provided essential insights into the crystal structure and phase composition of the cobalt doped manganese nanosystems, shedding light on the impact of varying doping levels and cobalt ion concentrations on the resulting material's properties. This information is crucial for understanding the structural behavior and potential applications of synthesized nanosystems in various scientific and technological fields [9, 13].

The energy dispersive X-ray spectrum of carbon with a % CO₂ doping, and pure manganese was analyzed in this study. Based on the positions of the spectrum's peaks for manganese, oxygen, and manganese-cobalt-oxygen elements, the processed sample was found to contain only manganese and

cobalt elements, respectively. This suggests that the nanomaterial created is clean and free from any further impurities [14]. The sol-gel technique used in the study plays a crucial role in maintaining the atoms or ions in their designated positions within molecules and crystals. These systems have the capability of vibrating, which is dependent on the components and type of bond used [15, 16]. The vibrational frequencies in such systems are influenced by the atomic weight of the constituent atoms and the strength of the bonding [14]. The findings from the energy dispersive X-ray spectrum and the discussion on the sol-gel technique provide important information about the composition and structural characteristics of the nanomaterial. This knowledge is valuable in understanding its properties and potential applications in various scientific and technological fields [17].

In the infrared experiment, light frequency is utilized to measure the intensity of an infrared beam's optical properties both before and after it interacts with a sample. The resulting plot of relative intensity vs frequency, as well as the halogen coating, are both examples of what is referred to as the "infrared spectrum." The Fourier transform technique is employed to convert the intensity-time output of the interferometer into the infrared spectrum. This process enables the visualization and analysis of the specific frequencies at which the sample interacts with the infrared light, providing valuable information about its chemical composition and molecular structure. Additionally, the study includes the SEM spectrum of cobalt doped manganese nanosystems. SEM is a powerful imaging technique that allows for the detailed visualization and analysis of the surface morphology and microstructure of the nanosystems, providing further insights into their characteristics and properties. Together, the infrared spectrum and SEM analysis provide a comprehensive understanding of the optical and microstructural properties of the cobalt doped manganese nanosystems, offering valuable data for their potential applications in various scientific and technological fields. Cobalt doped manganese nanoparticles are listed by functional groups in table 1. The results are in line with the literature in a significant way. The peaks at 500 and 600 cm⁻¹ denote the Mn-O stretching mode.

The produced samples, synthesized using the sol-gel method, were examined for their optical characteristics through hysteresis loops. Additionally, these samples possess several beneficial and distinctive qualities, including a wide specific surface area, good catalytic performance, nontoxicity, and abundance of natural elements. Notably, the samples also exhibit a narrow optical band gap. One significant challenge in

Table 4: Independent t-test for equality of means of the band gap (eV) values for the group. These results showed that there was a statistically significant difference between the two groups with the p-value is 0.000 (p < 0.05).

		Levene's test for equality of variances		T-test for equality of means						
		F	Sig.	t	df	Sig. (2-tailed)	Mean difference	Std. error difference	95% CI of the difference	
Band gap (eV)	Equal variance assumed	48.804	0	11.938	38	0.000	2.38850	0.20008	1.98347	2.79353
	Equal variance not assumed			11.938	19.747	0.000	2.38850	0.20008	1.97080	2.80620

the automotive industry is the issue of light-reflecting properties, which needs to be addressed effectively. As a result, the ongoing research aims to develop or enhance a technique that can overcome these optical limitations. By doing so, this material can be effectively utilized to separate solids from aqueous solutions, providing potential solutions to the challenges faced in this area. The combination of the unique properties and narrow optical band gap in the synthesized material makes it a promising candidate for various applications, including in catalysis, environmental remediation, and potentially addressing the light-reflecting properties in automobile vehicles. Further research and development in this area can lead to innovative solutions and practical applications to benefit various industries.

Conclusion

In this study, the band gap of novel manganese particles (20 wt.%), cobalt particles (5 wt.%), and halogen was investigated. The band gap of Mn-Co nanoparticles, with a mean eV of 0.7370 mm³/sec, was found to be 0.3568 mm³/sec higher than normal illumination. The t-test statistical analysis of the eV of activation energy revealed that the band gap energy was increased by 51% in the manganese doped with cobalt powder group ($t = 51.321 = 11.938$, $p = 0.001$). This indicates that the mean/average eV is significantly different between the material groups. The study concluded that the halogen coating material provides only normal lighting, while the sustainable Mn-Co nanoparticles exhibit enhanced optical properties. This suggests that the novel Mn-Co nanoparticles have the potential to improve their optical characteristics, making them a promising material for various applications where enhanced illumination properties are required. The findings of this study contribute to a deeper understanding of the optical properties of novel nanoparticles and highlight their potential for practical applications in various fields, including lighting and optical devices. Further research in this area may lead to the development of advanced materials with improved optical performance and efficiency.

Acknowledgements

None.

Conflict of Interest

The authors have not faced any conflicts and declare that this study is relevant to the content of the article.

References

1. Lei S, Tang K, Fang Z, Sheng J. 2007. One-step synthesis of colloidal Mn₃O₄ and γ-Fe₂O₃ nanoparticles at room temperature. *J Nanopart Res* 9: 833-840. <https://doi.org/10.1007/s11051-006-9131-4>
2. Park J, Kang E, Bae CJ, Park JG, Noh HJ, et al. 2004. Synthesis, characterization, and magnetic properties of uniform-sized MnO nanospheres and nanorods. *J Phys Chem B* 108(36): 13594-13598. <https://doi.org/10.1021/jp048229e>
3. Si PZ, Li D, Choi CJ, Li YB, Geng DY, et al. 2007. Large coercivity and small exchange bias in Mn₃O₄/MnO nanoparticles. *Solid State Commun* 142(12): 723-726. <https://doi.org/10.1016/j.ssc.2007.04.029>
4. Vázquez-Olmos A, Redón R, Fernández-Osorio AL, Saniger JM. 2005. Room-temperature synthesis of Mn₃O₄ nanorods. *Appl Phys A* 81: 1131-1134. <https://doi.org/10.1007/s00339-005-3291-4>
5. Zhang YC, Qiao T, Hu XY. 2004. Preparation of Mn₃O₄ nanocrystallites by low-temperature solvothermal treatment of γ-MnOOH nanowires. *J Solid State Chem* 177(11): 4093-4097. <https://doi.org/10.1016/j.jssc.2004.05.034>
6. Rohatgi A, Weber ER, Kimerling LC. 1993. Opportunities in silicon photovoltaics and defect control in photovoltaic materials. *J Electron Mater* 22: 65-72. <https://doi.org/10.1007/BF02665725>
7. Ahmad T, Ramanujachary KV, Lofland SE, Ganguli AK. 2004. Nanorods of manganese oxalate: a single source precursor to different manganese oxide nanoparticles (MnO, Mn₂O₃, Mn₃O₄). *J Mater Chem* 14(23): 3406-3410. <https://doi.org/10.1039/b409010a>
8. Hassan MS, Amna T, Pandeya DR, Hamza AM, Bing YY, et al. 2012. Controlled synthesis of Mn₂O₃ nanowires by hydrothermal method and their bactericidal and cytotoxic impact: a promising future material. *Appl Microbiol Biotechnol* 95: 213-222. <https://doi.org/10.1007/s00253-012-3878-6>
9. Zhang X, Yue L, Wan M, Zheng Y. 2010. Synthesis of porous manganese oxides bars via a hydrothermal-decomposition method. *Mater Chem Phys* 124(1): 831-834. <https://doi.org/10.1016/j.matchemphys.2010.07.068>
10. Francis TM, Lichty PR, Weimer AW. 2010. Manganese oxide dissociation kinetics for the Mn₂O₃ thermochemical water-splitting cycle. Part 1: experimental. *Chem Eng Sci* 65(12): 3709-3717. <https://doi.org/10.1016/j.ces.2010.03.002>
11. Makovec D, Drogenik M, Žnidaršič A. 2001. Sintering of MnZn-ferri-rite powders prepared by hydrothermal reactions between oxides. *J Eur Ceram Soc* 21(10-11): 1945-1949. [https://doi.org/10.1016/S0955-2219\(01\)00148-0](https://doi.org/10.1016/S0955-2219(01)00148-0)
12. Guinier A. 1994. X-ray Diffraction in Crystals, Imperfect Crystals, and Amorphous Bodies. Courier Corporation.
13. Midhun S, Ramesh C, Chellamuthu K, Yokeswaran R. 2022. Dissimilar resistance spot welding process on AISI 304 and AISI 202 by investigation metals. *Mater Today Proc* 69: 1213-1217. <https://doi.org/10.1016/j.matpr.2022.08.262>
14. Thota N, Reddy MV, Kumar A, Khan IA, Sangwan PL, et al. 2010. Substituted dihydronaphthalenes as efflux pump inhibitors of *Staphylococcus aureus*. *Eur J Med Chem* 45(9): 3607-3616. <https://doi.org/10.1016/j.ejmech.2010.05.006>
15. Yokeswaran R, Vijayan V, Karthikeyan T, Kumar BS, Kumar GS. 2019. Comprehensive analysis of surface modification process parameters by using tungsten inert gas welding process comprehensive analysis of surface modification process parameters by using tungsten inert gas welding process. *J New Mater Electrochem Syst* 22(1): 45-49.
16. Yokeswaran R, Chandran SS, Loganathan M, Veluchamy B. 2022. Influence of different insulation materials for effective cooling performance. *Mater Today Proc* 69: 967-973. <https://doi.org/10.1016/j.matpr.2022.07.417>
17. Yokeswaran R, Vijayan V, Karthikeyan T, Loganathan M, Antony AG. 2020. Microstructure analysis of IS2062 plates clad with SS2594 by TIG welding process. *J New Mater Electrochem Syst* 23(4): 269-273. <https://doi.org/10.14447/james.v23i4.a08>